Improved calculations of electron capture transitions for decay data and radionuclide metrology

Xavier Mougeot

Improved calculations of electron capture transitions for decay data and radionuclide metrology

X. Mougeot[a,*]

[a] CEA, LIST, Laboratoire National Henri Becquerel (LNE-LNHB), Bât. 602 PC111, CEA-Saclay 91191 Gif-sur-Yvette Cedex, France.

Abstract

Electron capture properties are crucial to establish the decay schemes of numerous radionuclides. The present modelling aims at improving the theoretical estimates of these decays, which are needed when no measurement is available. Allowed and forbidden unique transitions are calculated on the basis of precise relativistic wave functions of the atomic electrons, determined in previous work. In this context, correcting for atomic effects is of high importance. The two common approaches from Bahcall and Vatai to correct for the overlap and exchange effects have been extended to every subshell in a unified formulation, with the electron occupation precisely taken into account. The shake-up and shake-off effects, which create secondary vacancies, and the influence of the hole due to the capture process, have been considered. Uncertainties are also estimated. Relative capture probabilities and their ratios, including capture-to-positron ratios, have been found to be in good agreement with a selection of precise measurements. This modelling was then applied to the third forbidden unique transition of ^{40}K decay, with an update of the recommended values for the branching ratios and the total decay half-life.

* xavier.mougeot@cea.fr; tel. +33 (0)1 69 08 23 32; fax +33 (0)1 69 08 26 19

Keywords: Radionuclide metrology; decay data; electron capture; overlap and exchange effects; shake-up and shake-off effects; inner hole effect; ^{55}Fe; ^{138}La; ^{40}K.

1. Introduction

As a Designated Laboratory in charge of ionizing radiation metrology, the National Laboratory Henri Becquerel (LNE-LNHB) coordinates the evaluation of decay data within the international Decay Data Evaluation Project (DDEP) (Kellett and Bersillon, 2017), which aims at improving the fundamental knowledge of radionuclide decay schemes. The properties of electron capture transitions, such as capture probabilities and capture-to-positron probability ratios, are often pivotal information when establishing these decay schemes.

The capture process is very similar to beta decay, but instead of emitting an electron and an antineutrino, the nucleus absorbs an atomic electron and emits only a neutrino. Consequently, a ground-state to ground-state transition can only be detected through the subsequent atomic rearrangement, which makes precise measurements difficult to perform for low atomic number (Z) radionuclides. The theoretical calculations inherently depend on the precision of the atomic electron wave functions, for which a relativistic treatment is mandatory for high Z. Besides, as the nuclear structure component only acts as a constant factor in allowed transitions, ratios of electron capture probabilities are only sensitive to atomic properties and were therefore often measured to explore different atomic effects. The most complete survey of experimental and theoretical electron capture transitions was published 40 years ago (Bambynek et al., 1977).

The study of electron capture transitions is of importance in radionuclide metrology, fundamental physics and for many applications such as nuclear astrophysics and cosmochronology, absolute geochronology, nuclear medicine and nuclear energy. Regarding radionuclide metrology, the modelling of the light emission in activity measurements carried

out by the Liquid Scintillation Counting (LSC) technique is sensitive to the number of emitted particles at low energy (Broda et al., 2007). For radionuclides decaying by electron capture, the LSC technique requires a precise modelling of the atomic rearrangement with a specific treatment for each of the different subshells. Hence, the capture probability is required for every subshell as this process creates the initial vacancies.

Investigating the ENSDF (Evaluated Nuclear Structure Data File) database (NNDC, 2017), which includes every known radionuclide, more than 35 000 beta or electron capture transitions can be found in more than 1 500 radionuclides, split into 35% beta minus, 28% beta plus and 37% electron capture. It should be noted that decay data evaluations must rely on theoretical predictions when experimental data are missing. Any calculation code has thus to provide precise estimates in a wide range of cases. In modern decay data evaluations, the LogFT (LogFT, 2001) and EC-capture (Schönfeld, 1998) programs are commonly used for determining capture probabilities. However, these codes are limited by their models and the capture probabilities can only be obtained for the inner atomic shells.

The LogFT program calculates allowed, first and second forbidden unique transitions and also treats the beta plus component, if any (LogFT, 2001). The fraction per electron capture decay is determined for the K, L, and M_+ shells, where M_+ denotes the cumulative probability of the higher shells. It is noteworthy that these capture probabilities are not relative but absolute, that is to say $P_K + P_{L_1} + \cdots \neq 1$. In fact, $\sum_i P_i = I_\varepsilon/(I_\varepsilon + I_{\beta^+})$, where I_ε is the absolute intensity of the electron capture branch and I_{β^+} is the absolute intensity of the competing beta plus branch. The probability ratios P_{L_2}/P_{L_1}, P_{L_3}/P_{L_1}, $P_\varepsilon/P_{\beta^+}$ and P_K/P_{β^+} are also determined. Uncertainties are propagated from the input parameters and an arbitrary modelling uncertainty of 1% is added for the total capture-to-positron ratio $P_\varepsilon/P_{\beta^+}$. Any final uncertainty less than 0.1% is not given by the LogFT program. The calculation assumes closed shells and is based on tabulated values of the radial densities at the nuclear surface of the electron wave functions,

corrected for atomic overlap and exchange effects (Martin and Blichert-Toft, 1970). The atomic wave function parameters were determined using a relativistic Hartree-Fock-Slater self-consistent approach and a realistic Fermi-Dirac distribution for the nuclear charge density (Lu et al., 1971).

The EC-capture program calculates relative capture probabilities for allowed transitions and claims to calculate first forbidden non-unique ones (Schönfeld, 1998). However, they are actually treated as allowed, since the nuclear structure is not taken into account. Relative probabilities for K, L, M, N and O shells are given with uncertainty propagation. The calculation assumes closed shells and is based on tabulated ratios of the bound wave functions evaluated at the nucleus. The wave functions are from a relativistic modelling and the ratios are those given in (Bambynek et al., 1977) for a small set of atomic numbers. The overlap and exchange correction is based on different models for low and high Z using the tabulated values given in (Bambynek et al., 1977), again for a small set of atomic numbers. Interpolation was used by the authors to complete each table for all Z.

Due to these limitations, information is missing for the user. To improve the situation, the modelling developed in this work relies on relativistic bound wave functions of the atomic electrons calculated specifically for the radionuclides involved in the considered transition. Probabilities and their ratios are thus accessible for any subshell. This physical modelling is described in Section 2, for which good agreement with the existing codes can be expected for allowed transitions. A comparison with experimental data is shown in Section 3 for a selection of allowed transitions. Forbidden unique transitions have also been considered, but only very few measurements are available in the literature. Finally, this modelling was applied to the third forbidden unique transition that occurs in the ^{40}K decay in order to update the decay scheme with the deduced branching ratios, which in turns modifies the evaluation of the total half-life.

2. A consistent formalism for electron captures

By its very nature, electron capture decay highly depends on the atomic structure of the radionuclides involved. Precise theoretical predictions require precise bound state wave functions and it is well-known that a relativistic modelling is mandatory for atomic numbers $Z \gtrsim 50$. A bound state is labelled by a set of two quantum numbers (n, κ) and the notation $x = (n, \kappa)$ is introduced to simplify the notations where no ambiguity is possible. A wave function is symbolised by $|(n, \kappa)\rangle$ or $|(n, \kappa)'\rangle$ in the parent or daughter atom respectively. Atomic energy, radial dependency, occupation number N_x and Coulomb amplitude β_x are necessary for each bound wave function. In the present work, the relativistic electron bound wave functions determined in (Mougeot and Bisch, 2014) for the precise calculation of the exchange effect in beta decays have been used.

The constants used throughout this work are α, the fine structure constant; m_e, the electron rest mass; c, the speed of light; $\hbar$, the reduced Planck's constant; and G_β, the Fermi constant. Natural units $\hbar = m_e = c = 1$ are applied in the present modelling. The nuclear radius is the usual one, $R = 1.2\, A^{1/3}$ fm, with A the mass number of the radionuclide.

Electron capture is an isobaric process which can compete with beta plus decay

$$\begin{aligned} (\varepsilon): \quad & {}^{A}_{Z}X + e^- \longrightarrow {}^{A}_{Z-1}Y + \nu_e \\ (\beta^+): \quad & {}^{A}_{Z}X \longrightarrow {}^{A}_{Z-1}Y + e^+ + \nu_e \end{aligned} \tag{1}$$

The available energy for the transition is determined from the Q-value and the energies of the initial and final nuclear states as $E_{\max} = Q + E_i - E_f$, and the total normalized energy is $W_0 = (1 + E_{\max}/m_e) - 2$. The recoil energy of the nucleus is neglected, as the largest known recoil occurs in ^{7}Be decay and is of 57 eV. A beta plus transition is only possible if $E_{\max} \geq 2m_e$ and the maximum energy of the beta spectrum is then $E_{\beta^+} = E_{\max} - 2m_e$. The energy E_x of an orbital is by definition negative and $W_x = 1 - |E_x|/m_e$ is the corresponding total energy. The

momentum of the neutrino particle, assumed to be massless, is $q_x = W_0 + W_x$ and the momentum of the captured electron is $p_x = \sqrt{1 - W_x^2}$.

2.1 Transition probabilities

Unlike beta decay, electron capture is a two-body process where particle energies are well-defined. However, the weak interaction acts in a very similar manner and a symmetry exists between both formalisms. A decay occurs from an initial nuclear state of the parent nucleus with spin and parity (J_i, π_i) to a final nuclear state (J_f, π_f) of the daughter nucleus. Transitions are classified as for beta decay on account of spin change $|\Delta J| = |J_i - J_f|$ and parity change $\pi_i \pi_f$. The formalism with spherical symmetry from (Behrens and Bühring, 1982) was followed throughout this work.

The total decay rate of a given transition is given by

$$\lambda_\varepsilon = \frac{\ln 2}{t_\varepsilon} = \frac{G_\beta^3}{2\pi^3} \sum_x n_x C_x f_x \tag{2}$$

where the partial half-life is defined from the total half-life and the branching ratio as $t_\varepsilon = T_{1/2}/P_\varepsilon$. The degeneracy of the orbital is $2k_x$, where $k_x = |\kappa|$, and n_x is the relative occupation number defined as $n_x = N_x/2k_x$ from the number of electrons N_x in the orbital. The quantity C_x plays a role similar to the shape factor in beta decay and the nuclear matrix elements ${}^A F^0_{L,L-1,1}$ are also, to a first approximation, independent of the lepton energy for allowed and forbidden unique transitions. Its expression can be found in (Bambynek et al., 1977)

$$C_x = \frac{(2L-2)!!}{(2L-1)!!} \left[{}^A F^0_{L,L-1,1} \right]^2 R^{2(L-1)} \frac{p_x^{2(k_x-1)} q_x^{2(L-k_x)}}{(2k_x-1)!\,[2(L-k_x)+1]!} \tag{3}$$

with $L = 1$ if $\Delta J = 0$ for an allowed transition and $L = \Delta J$ for any $(L\text{–}1)^{\text{th}}$ forbidden unique transition. The sum in Eq. (2) is limited by the L value such that $k_x = 1, 2, \ldots L$. Finally, the quantity f_x corresponds to the integrated Fermi function in beta decay and is defined as

$$f_x = \frac{\pi}{2} q_x^2 \beta_x^2 B_x \tag{4}$$

where B_x stands for the overlap and exchange correction, which is described in the next Section, and β_x is the Coulomb amplitude of the wave function.

The usual method to avoid the calculation of the nuclear matrix elements is to determine the relative capture probabilities P_x by: *i*) using the K capture as a reference; *ii*) noting that $\lambda_x/\lambda_K = P_x/P_K$; and *iii*) using the relation $\sum_x P_x = 1$. First determining the bound-state wave functions of the atomic electrons in both the parent and the daughter atoms, the ratio P_x/P_K is then calculated for each orbital and P_K is established using

$$P_K \left[1 + \sum_{\substack{x \\ x \neq K}} \frac{P_x}{P_K} \right] = 1 \tag{5}$$

Therefore, relative capture probabilities and their ratios are accessible for each subshell in the present modelling.

2.2 Overlap and exchange effects

Atomic effects in electron capture decays have been proven for a long time to be of high importance. J. N. Bahcall was the first to comprehensively study the underlying mechanisms (Bahcall, 1962), which come from the indistinguishability of the electrons and from the decrease of the nuclear charge by one unit during the decay.

To zeroth order, the atomic electrons which are not directly involved in the capture process can be considered as spectators, thus their contribution to the capture probability can be neglected. However, the change of the nuclear charge leads to an imperfect overlap $\langle (n,\kappa)' | (n,\kappa) \rangle$ between the initial and final atomic states and the cumulative imperfection for all the spectator electrons is not negligible at all. This is the so-called overlap effect.

Electrons being indistinguishable, the captured electron does not necessarily come from the orbital where the vacancy appears. For instance in a K capture, this can be seen as a virtual process where an electron from a higher orbital is captured and a K electron is promoted to this orbital. The final state, a vacancy in the K shell, is then identical to a direct K capture and cannot be distinguished experimentally. This is the so-called exchange effect, which depends on asymmetric overlaps $\langle(m,\kappa)'|(n,\kappa)\rangle$.

As emphasized by J. N. Bahcall in (Bahcall, 1965), the major difficulty for quantitative estimates of the atomic matrix elements is due to the shake-off effect: an infinite number of final atomic states significantly contribute to the decay probability. Bahcall's approach overcomes this difficulty by only considering the contribution of the 1s, 2s and 3s orbitals. This means that *i*) atomic electrons are separated into "inner" and "outer" electrons; *ii*) inner electrons are supposed to be almost inert; and *iii*) outer electrons are supposed to form a complete set of states. Moreover, the transition energy is assumed to be independent of the outer electrons in the final state due to their very small binding energies. The sum over the infinite states is performed using the closure property. The electron capture rate is then corrected by the quantity

$$B_i = \left|\frac{f_i}{\psi_i(0)}\right|^2 \tag{6}$$

with $\psi_i(r)$ the bound wave function. The three capture amplitudes f_i considered by Bahcall are

$$\begin{aligned} f_{1s'} = {} & \langle 2s'|2s\rangle\langle 3s'|3s\rangle\psi_{1s}(0) - \langle 2s'|1s\rangle\langle 3s'|3s\rangle\psi_{2s}(0) \\ & - \langle 3s'|1s\rangle\langle 2s'|2s\rangle\psi_{3s}(0) \end{aligned} \tag{7}$$

and $f_{2s'}$ and $f_{3s'}$ are obtained from $f_{1s'}$ by permutation ($1s \leftrightarrow 2s$, $1s' \leftrightarrow 2s'$; and $1s \leftrightarrow 3s$, $1s' \leftrightarrow 3s'$, respectively). This non-relativistic approach tends to underestimate the overlap correction and to overestimate M/L_1 capture ratios (Bambynek et al., 1977). Exchanges between inner and outer electrons are neglected, as well as multiple exchange processes and the effect of the vacancy in the daughter atomic cloud.

Another approach was developed by E. Vatai in (Vatai, 1970). The exchange correction was extended up to the 4s orbital and the overlap correction was more precisely defined by taking into account the contribution of every subshell. The corresponding capture amplitude for the K-shell is then

$$\begin{aligned} f_{1s'} = {} & \psi_{1s}(0)\langle 2s'|2s\rangle\langle 3s'|3s\rangle\langle 2p'|2p\rangle \ldots \\ & - \psi_{2s}(0)\langle 2s'|1s\rangle\langle 3s'|3s\rangle\langle 2p'|2p\rangle \ldots \\ & - \psi_{3s}(0)\langle 3s'|1s\rangle\langle 2s'|2s\rangle\langle 2p'|2p\rangle \ldots \\ & - \psi_{4s}(0)\langle 4s'|1s\rangle\langle 2s'|2s\rangle\langle 2p'|2p\rangle \ldots \end{aligned} \tag{8}$$

and the other f_i can be obtained by permutation as in Bahcall's approach. Vatai also highlighted the influence of the vacancy created by the capture process on the orbitals of the daughter atom. However, multiple exchange processes are not considered, as in Bahcall's approach. This non-relativistic approach tends to underestimate L/K capture ratios at low Z (Bambynek et al., 1977).

Both approaches were unified and improved in the present modelling within a relativistic formalism in order to reach reliable predictions for both low and high Z radionuclides. The overlap and exchange correction for a captured electron in an (n, κ) orbital is defined as

$$B_{n\kappa} = \left|\frac{b_{n\kappa}}{\beta_{n\kappa}}\right|^2 \tag{9}$$

with $\beta_{n\kappa}$ the Coulomb amplitude of the wave function. The quantity $b_{n\kappa}$ has been mathematically derived and established to be

$$\begin{aligned} b_{n\kappa} = t_{n\kappa}\left[\prod_{m\neq n}\langle (m,\kappa)'|(m,\kappa)\rangle\right]\Bigg[\beta_{n\kappa} \\ - \sum_{m\neq n}\beta_{m\kappa}\frac{\langle (m,\kappa)'|(n,\kappa)\rangle}{\langle (m,\kappa)'|(m,\kappa)\rangle}\Bigg] \end{aligned} \tag{10}$$

with $t_{n\kappa} = 1$ for the generalized Bahcall approach. For the generalized Vatai's approach, the following formula has been obtained

$$t_{n\kappa}$$

$$= \langle (n,\kappa)' | (n,\kappa) \rangle^{n_{n\kappa}-1/2|\kappa|} \left[\prod_{m \neq n} \langle (m,\kappa)' | (m,\kappa) \rangle^{n_{m\kappa}-1} \right] \left[\prod_{\substack{m,\mu \\ \mu \neq \kappa}} \langle (m,\mu)' | (m,\mu) \rangle^{n_{m\mu}} \right] \quad (11)$$

The degeneracy of the orbitals and the disappearance of the captured electron are correctly taken into account. Exchange with all other electrons of identical κ is considered, exchange with electrons of different κ being forbidden. Every bound state is considered in the overlap correction. In the following Sections, the present modelling is modified in order to account for shaking and hole effects.

2.3 Shake-up and shake-off effects

Shake-up (internal excitation) and shake-off (internal ionization) create secondary vacancies in the atomic cloud and are usually treated as time-independent processes in the "sudden" approximation. The use of closure in Bahcall's approach for determining the overlap and exchange correction inherently accounts for shake-up and shake-off, but overestimates these effects. Vatai's approach simply neglects these shaking effects. In this work, Vatai's approach has been complemented with an approximate estimate of the emission probability of secondary electrons for each possible captured electron, following the formulation from (Crasemann et al., 1979).

In principle, the calculation of the shake-off effect requires determining the overlap between the bound wave function of the ejected electron in the potential of the parent atom and the continuum wave function of this electron in the potential of the daughter atom. To overcome these ponderous calculations, interest is only focused on the estimate of both shake-up and shake-off at once. Indeed, each electron has only three possibilities in the final state: *i*) remaining in its original state; *ii*) being excited to an unoccupied state (shake-up); and *iii*) being ionized to the continuum (shake-off). The shaking probability can thus be obtained by

subtracting from unity the probability that the electron retains its original quantum numbers. However, the Pauli principle prohibits atomic transitions to occupied bound states and this contribution has also to be removed. The shaking probability for an electron in an (m,κ) orbital is then

$$P_{m\kappa} = 1 - |\langle (m,\kappa)'|(m,\kappa)\rangle|^{2n_{m\kappa}} - \sum_{l\neq m} n'_{l\kappa} n_{m\kappa} |\langle (l,\kappa)'|(m,\kappa)\rangle|^2 \qquad (12)$$

where the number of electrons in a given shell used in (Crasemann et al., 1979) has been replaced by the corresponding relative occupation number for the sake of consistency with the Behrens and Bühring formalism.

For each captured electron in an (n,κ) state, the probability of a regular capture, which leads to one vacancy in the final state, has to be summed with the probability of two vacancies in the final state, one from the capture and the second from the shaking process. That is to say

$$\lambda_{n\kappa} \longrightarrow \lambda_{n\kappa}\left(1 + \sum_{m,\kappa} P_{m\kappa}\right) \qquad (13)$$

As the present modelling relies on the calculation of capture probability ratios, the accuracy of the total shaking emission probability per capture is less important than the accuracy of the relative shaking probability between two subshells. However, the shaking contribution is fully involved in capture-to-positron ratios (see Sec. 2.5) and its accuracy is then of importance.

2.4 Inner hole effect

Up-to-now, a neutral daughter atom has been considered in the present modelling with orbitals filled according to the Madelung rule. However, the electron capture process creates a vacancy in a shell of the parent atom and decreases the atomic number by one unit. The daughter atom is thus overall neutral, but the atomic configuration no longer follows the Madelung rule, being equivalent to the promotion of the captured electron to the valence orbital.

This effect mainly occurs in the inner shells as K and L captures are dominant. Taking into account the so-called "inner hole effect" is not straightforward. Omitting the contribution of the captured electron in the final configuration is not sufficient. The disappearance of its charge modifies the energy and the wave function of the other atomic orbitals. An exact treatment can only be done through a relativistic self-consistent method, which is far beyond the scope of the present work. As suggested by Vatai, (1970), approximate wave functions of the excited daughter atom can be obtained by means of first order, time-independent perturbation theory. Starting from the Hamiltonian $\mathcal{H}_0$ of the parent atom, the wave function of an $(i,\kappa)'$ orbital of the daughter atom is determined using a perturbing Hamiltonian $\mathcal{H}'$ which results from the change of the nuclear charge and the removal of the mean influence of the captured electron (n,κ)

$$(\mathcal{H}_0 + \mathcal{H}')|(i,\kappa)'\rangle = (E_0 + E')|(i,\kappa)'\rangle \tag{14}$$

$$\mathcal{H}' = \frac{\alpha}{r} - \langle(n,\kappa)|\frac{\alpha}{|\overrightarrow{r_{n\kappa}} - \vec{r}|}|(n,\kappa)\rangle \tag{15}$$

A daughter orbital then results from the corresponding parent eigenstate corrected by a perturbation which mixes this state with the other eigenstates

$$|(i,\kappa)'\rangle = |(i,\kappa)\rangle - \sum_{j\neq i}\frac{\langle(j,\kappa)|\mathcal{H}'|(i,\kappa)\rangle}{W_j - W_i}|(j,\kappa)\rangle \tag{16}$$

The coupling between eigenstates with different κ is null due to the orthogonality of the wave functions. The present modelling only requires overlaps of the wave functions. With perturbation theory, a symmetric overlap $\langle(i,\kappa)'|(i,\kappa)\rangle$ would be strictly equal to unity. The correction of the hole effect is thus only applied through the asymmetric overlaps

$$\langle(j,\kappa)'|(i,\kappa)\rangle = \frac{\langle(j,\kappa)|\mathcal{H}'|(i,\kappa)\rangle}{W_j - W_i} \tag{17}$$

Starting from the analysis in (Messiah, 1995) and noticing that the quantity $\langle(j,\kappa)|\mathcal{H}'|(i,\kappa)\rangle$ reduces to its radial part because of the spherical symmetry of the problem, one obtains after some calculations

$$\langle(j,\kappa)|\mathcal{H}'|(i,\kappa)\rangle = \int_0^\infty (\alpha r)\left[f_{j\kappa}(r)f_{i\kappa}(r) + g_{j\kappa}(r)g_{i\kappa}(r)\right] \times \left\{1 - \int_0^r x^2[g_{n\kappa}^2(x) + f_{n\kappa}^2(x)]\mathrm{d}x - r\int_r^\infty x[g_{n\kappa}^2(x) + f_{n\kappa}^2(x)]\,\mathrm{d}x\right\}\mathrm{d}r \tag{18}$$

2.5 Electron-capture to positron-decay ratios

Provided that $E_{\max} \geq 2m_e$, a beta plus transition can compete with an electron capture. Then, the ratio of capture-to-positron probabilities is determined for each orbital as

$$\frac{\lambda_x}{\lambda_{\beta^+}} = \frac{n_x C_x f_x}{f_{\beta^+}} \tag{19}$$

and the total capture-to-positron ratio results from the summation of the individual ratios

$$\frac{\lambda_\varepsilon}{\lambda_{\beta^+}} = \frac{\sum_x n_x C_x f_x}{f_{\beta^+}} \tag{20}$$

The integrated positron spectrum f_{β^+} takes into account the shape factor according to the forbiddenness of the transition. It is noteworthy that the constant part, which includes the nuclear matrix elements, is identical for both the beta plus and the electron capture decays for allowed and forbidden unique transitions. For the sake of consistency, f_{β^+} is calculated considering that the positron feels the same atomic screened potential as the atomic electrons, as described in detail in (Mougeot and Bisch, 2014). This method slows down the computation of the spectrum but ensures the precise calculation of electron-capture to positron-decay ratios.

2.6 Uncertainties

As the input parameters are only the Q-value and the initial and final nuclear level energies, the propagation of their uncertainties only results in an uncertainty on $E_{\max}$. Since P_K is clearly correlated to the other relative probabilities, the most appropriate method which inherently accounts for this correlation is to perform the calculation three times at $E_{\max} - u(E_{\max})$, $E_{\max}$ and $E_{\max} + u(E_{\max})$. The uncertainties of the input parameters being standard deviations, the uncertainty of a calculated quantity A is consistently determined by

$$u(A) = \max\left(\frac{|A_{\max} - A_{\min}|}{2}, |A - A_{\min}|, |A - A_{\max}|\right) \tag{21}$$

In principle, for small uncertainties, each term on the right side of this equation should be identical.

Each quantity is determined following two different models: *i*) extended Bahcall's approach with hole effect; and *ii*) extended Vatai's approach with hole and shaking effects. The results from these two models differ by more than the propagated uncertainty, except for large $u(E_{\max})$. Besides that, the improvements that were implemented for each approach in the present work make it difficult to predict which one is the most accurate for a given transition. Therefore, the final calculated quantity is the simple mean of the results from Bahcall's and Vatai's improved approaches. The final uncertainty is determined as explained above via Eq. (21).

The reliability of this uncertainty assessment is difficult to estimate. Other components are not considered because they would require comparisons with other models of high precision: atomic energies and Coulomb amplitudes of the wave functions; overlaps; shaking effects; hole effect and forbidden corrections to the C_x factor. The present uncertainty could thus be considered as underestimated. However, the difference between the results from Bahcall's and Vatai's approaches introduces a large uncertainty while, in principle, only the most precise approach should be considered.

3. Validation

The validation of the physical modelling presented in the previous Section can only be done through comparison with measurements. However, high precision measurements of electron capture transitions are challenging. The recoil of the nucleus could be measured, but the largest known recoil occurs for the lightest nucleus that decays through electron capture, ^{7}Be, and is only 57 eV. As the detection of neutrinos is definitely not appropriate, electron capture rates can only be determined from the subsequent atomic and nuclear radiations. For ground-state to ground-state transitions, only atomic radiations are detectable, which can be difficult for low-mass radionuclides. The most reliable information then comes from the measurement of capture probability ratios, such as P_L/P_K or P_M/P_L, and capture-to-positron probability ratios if energetically possible, such as $P_\varepsilon/P_{\beta^+}$ or P_K/P_{β^+}. The notations are usually simplified as L/K, M/L, ε/β^+, K/β^+, etc. A complete and careful survey can be found in (Bambynek et al., 1977). The theoretical predictions from the present work have been compared to measurements that mainly come from this survey, with an update of the Q-values from (Wang et al., 2017), the nuclear level energies from (NNDC, 2017) and taking into account new measurements. The selected transitions were chosen to span over a wide range in Z and to test different forbiddennesses.

3.1 Allowed transitions

Most of the measured values available in the literature are from allowed capture transitions. Those selected for comparison with the theoretical predictions range from $Z = 6$ to $Z = 56$. It should be noted that the LogFT program does not provide any uncertainty on the K/β^+ ratio and that the EC-capture program does not treat beta plus transitions. Table 1 presents the comparison for seven allowed transitions from the decays of ^{11}C, ^{22}Na and ^{65}Zn (capture-to-positron ratios) and of ^{55}Fe and ^{133}Ba (capture probability ratios).

Table 1. Comparison between measured and calculated probability ratios from the LogFT and EC-capture programs and the present work, for allowed electron capture transitions. The measured values can be found in (Bambynek et al., 1977), and in (Bé et al., 2005) for ^{65}Zn. Results from this work under different assumptions are in italics.

Nuclide		Prob. ratio	Experiment	This work	LogFT	EC-capture
	This work	*Bahcall (no hole)*	*Bahcall*	*Vatai (no hole, no shake)*	*Vatai (no shake)*	*Vatai*
^{11}C		$K/\beta^+{}_{\mathrm{WM}}$[1]	0.00225 (15)	0.00218 (8)	0.002228	–
	This work	*0.00207*	*0.00210*	*0.00196*	*0.00199*	*0.00226*
^{22}Na		$\varepsilon/\beta^+{}_{\mathrm{UWM}}$[1]	0.1083 (9)	0.1143 (10)	0.1117 (11)	–
	This work	*0.1124*	*0.1134*	*0.1086*	*0.1096*	*0.1152*
		K/β^+	0.105 (9)	0.1058 (9)	0.1031	–
	This work	*0.1042*	*0.1050*	*0.1007*	*0.1014*	*0.1067*
^{55}Fe		L/K_{WM}[1]	0.1165 (12)	0.11823 (30)	0.1101	0.1111 (15)
	This work	*0.11951*	*0.11853*	*0.11935*	*0.11838*	*0.11793*
		M/L_{WM}[1]	0.1556 (26)	0.1708 (12)	0.1683[2]	0.160 (6)
	This work	*0.1641*	*0.1714*	*0.1639*	*0.1712*	*0.1701*
		M/K_{WM}[1]	0.0178 (6)	0.02019 (13)	0.0185[2]	0.0177 (7)
	This work	*0.01961*	*0.02032*	*0.01956*	*0.02027*	*0.02006*
^{65}Zn		$K/\beta^+{}_{\mathrm{WM}}$[1]	30.1 (5)	29.8 (6)	30.03	–
	This work	*29.19*	*29.35*	*27.85*	*28.00*	*30.32*
^{133}Ba (437 keV)		L/K	0.371 (7)	0.375 (8)	0.374 (7)	0.376 (6)
	This work	*0.370*	*0.376*	*0.369*	*0.376*	*0.374*
^{133}Ba (384 keV)		L/K	0.221 (5)	0.2265 (18)	0.2271 (9)	0.2277 (20)
	This work	*0.2231*	*0.2272*	*0.2226*	*0.2267*	*0.2258*

1. (Un-)Weighted mean of several measurements (see text).
2. A contribution of 4% for the N_1 shell estimated with the EC-capture program has been removed.

The ^{11}C decay is a ground-state ($3/2^-$) to ground-state ($3/2^-$) transition where the pre-eminent component is beta plus emission. The experimental ratio K/β^+ corresponds to the weighted mean of two measurements given in (Bambynek et al., 1977). Excellent agreement is

obtained from the present modelling and the LogFT program, the latter providing no uncertainty.

The ^{22}Na decay is highly dominated by the allowed transition from its ground state (3^+) to the first excited state (2^+, 1274.5 keV) of ^{22}Ne. The ε/β^+ ratio was initially measured in order to test for the existence of Fierz interference, but great discrepancies between the experimental results ruled out any firm conclusion (Firestone et al., 1978). Indeed, this measurement is delicate as X-rays and Auger electrons are emitted at very low energy, below 1 keV, which greatly complicates any direct measurement of the electron capture probabilities. Measurements given in (Bambynek et al., 1977) and (Galán, 2009) have been considered and are shown in Figure 1. In this discrepant set of 16 data, the two highest values are excluded by Chauvenet's criterion and the mean value of $\varepsilon/\beta^+ = 0.1083\ (9)$ is an unweighted average. A single measurement of $K/\beta^+ = 0.105\ (9)$ can also be found in (Bambynek et al., 1977). The K/β^+ ratio from this work is found in better agreement compared to LogFT, but the large uncertainty of the measurement cannot allow ruling out LogFT result. The well-known discrepancy between experiment and theory for the ε/β^+ ratio is still present, with worse agreement with the measurement compared to LogFT. This situation motivates new high precision measurements as well as theoretical improvements.

Focus is now made on the ^{65}Zn transition where the beta plus process competes with electron capture. This ground-state ($5/2^-$) to ground-state ($3/2^-$) transition is highly dominated by electron capture. From the seven measurements found in (Bambynek et al., 1977) and (Bé et al., 2005), a weighted mean of $K/\beta^+ = 30.1\ (5)$ was derived. The calculated values from both this work and LogFT are in excellent agreement.

Figure 1. Experimental values of the total capture-to-positron ratio for the main allowed transition in ^{22}Na decay. The NSR key-numbers which correspond to the publications are given on the abscissa (Pritychenko et al., 2011).

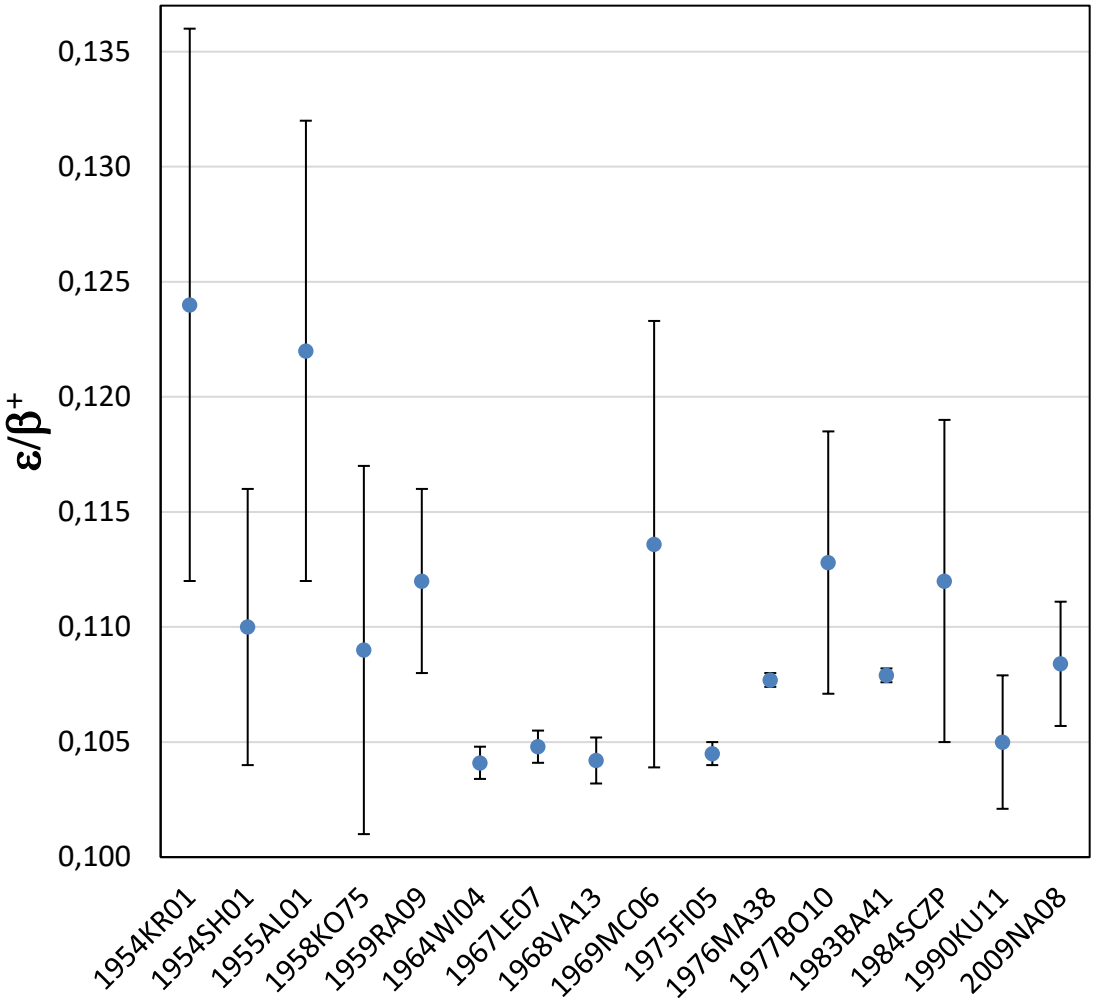

Another difficult measurement is the ^{55}Fe decay as the Q-value is too low for beta plus emission and the atomic emissions are below 7 keV. This transition is ground-state (3/2$^-$) to ground-state (5/2$^-$) and the experimental L/K and M/L ratios from a single measurement can be found in (Bambynek et al., 1977), from which the experimental M/K ratio has been deduced. The very recent measurement using metallic magnetic calorimetry (Loidl and Rodrigues, 2017) should also be taken into account. The final values in Table 1 correspond to the weighted means of these two measurements. The EC-capture program provides capture probabilities with uncertainties for K, L, M and N shells, which allows comparing the L/K, M/L and M/K ratios with the calculated values from this work. On the other hand, the LogFT program provides capture probabilities without any uncertainty for this transition and, removing the N shell

contribution estimated with EC-capture, comparison is also possible for the M/L and M/K ratios. The present modelling is the only one that is almost consistent with the measured L/K ratio due to a smaller K capture probability. However, the agreement is worse for M/L and M/K, which is most probably due to excessive corrections for the M unclosed shell.

The two principal electron capture transitions in the ^{133}Ba decay have also been investigated. For both of them, only a single measurement of the L/K ratio was found. These ratios are given in (Bambynek et al., 1977). The main transition occurs between the ground state ($1/2^+$) of ^{133}Ba to the fourth excited-state ($1/2^+$, 437 keV) of ^{133}Cs. All three theoretical models provide values consistent with the experimental L/K ratio. The second transition being considered is to the third excited state ($3/2^+$, 383.8 keV) of ^{133}Cs. Theoretical predictions from this work and EC-capture are consistent with the experimental L/K ratio.

3.2 Forbidden unique transitions

Firstly, it must be noted that the EC-capture program cannot calculate forbidden unique transitions, hence results from this work can only be compared with those from the LogFT program and from measurements. However, the relevance of this comparison is severely limited by the very small number of measurements that have been published.

Table 2 presents this comparison for six first forbidden unique transitions from the electron capture decay of the following radionuclides: ^{81}Kr; ^{84}Rb; ^{122}Sb; ^{126}I; ^{202}Tl and ^{204}Tl. In most cases, except for ^{204}Tl decay, only a single measurement is available. For ^{204}Tl decay, the measurements cited in (Bambynek et al., 1977) and (Bé and Chisté, 2003) have been considered and a weighted mean determined. Except for ^{204}Tl, results from this work are consistent with the measurements, even if the large experimental uncertainty should be underlined. For four out of the six cases, LogFT does not provide any uncertainty. A slight tendency can be observed where the present modelling provides values closer to the experimental ones.

Table 2. Comparison between measured and calculated probability ratios from the LogFT program and the present work, for first forbidden unique electron capture transitions. All transitions are ground-state to ground-state and $2^- \rightarrow 0^+$, except for ^{81}Kr which is $7/2^+ \rightarrow 3/2^-$. The measured values can be found in (Bambynek et al., 1977). Results from this work under different assumptions are in italics.

	Nuclide	Prob. ratio	Experiment	This work	LogFT
This work	*Bahcall (no hole)*	*Bahcall*	*Vatai (no hole, no shake)*	*Vatai (no shake)*	*Vatai*
	^{81}Kr	L/K	0.146 (5)	0.14851 (37)	0.15001 (10)
This work	*0.146*	*0.149*	*0.146*	*0.147*	*0.148*
	^{84}Rb	K/β^+	1.12 (25)	0.905 (13)	0.9004
This work	*0.894*	*0.896*	*0.784*	*0.787*	*0.914*
	^{122}Sb	K/β^+	300 (50)	256 (10)	249.7
This work	*251*	*252*	*237*	*238*	*259*
	^{126}I	K/β^+	20.2 (20)	20.38 (47)	19.85
This work	*20.11*	*20.19*	*19.01*	*19.09*	*20.56*
	^{202}Tl	L/K_{sym}[1]	0.223 (18)	0.2105 (5)	0.2113
This work	*0.2104*	*0.2109*	*0.2098*	*0.2103*	*0.2100*
	^{204}Tl	L/K_{WM}[2]	0.47 (3)	0.5150 (49)	0.5196 (19)
This work	*0.5132*	*0.5173*	*0.5095*	*0.5135*	*0.5128*

1. Measured value given with asymmetric uncertainties and symmetrized following (Audi et al., 2012).
2. Weighted mean of several measurements (see text).

Only two second forbidden unique transitions have been measured. The first one is the main decay of ^{26}Al, from its ground-state (5^+) to the first excited state (2^+, 1808.7 keV) of ^{26}Mg. The measurement given in (Bambynek et al., 1977) is known to be underestimated since the reinvestigation of Samworth et al. (1972) who carefully determined $\varepsilon/\beta^+ = 0.185\ (44)$. This work yields a result in excellent agreement but the large uncertainty of the measurement does not exclude the LogFT result (see Table 3).

The improvement of the present modelling is more visible with the main decay of ^{138}La, from its ground-state (5^+) to the first excited state (2^+, 1435.8 keV) of ^{138}Ba. The measured probability ratios from (Quarati et al., 2016) are compared with the results from LogFT and this work in Table 3. The M/K and M/L ratios from this work are remarkably consistent with the measurement while LogFT does not provide useful information for the M shell. However, the L/K ratio from this work is not so close to the measured one, but is still better than the result from LogFT.

Table 3. Comparison between measured and calculated probability ratios from the LogFT program and the present work, for second forbidden unique electron capture transitions. The measured values are from (Quarati et al., 2016) for ^{138}La and from (Samworth et al., 1972) for ^{26}Al. Results from this work under different assumptions are in italics.

	Nuclide	Prob. ratio	Experiment	This work	LogFT
This work	*Bahcall (no hole)*	*Bahcall*	*Vatai (no hole, no shake)*	*Vatai (no shake)*	*Vatai*
	^{138}La	L/K	0.391 (3)	0.416 (8)	0.427 (5)
This work	*0.413*	*0.418*	*0.411*	*0.416*	*0.415*
		M/K	0.102 (3)	0.1045 (24)	–[1]
This work	*0.1049*	*0.1052*	*0.1043*	*0.1046*	*0.1037*
		M/L	0.261 (9)	0.251 (8)	–[1]
This work	*0.254*	*0.252*	*0.254*	*0.251*	*0.250*
	^{26}Al	ε/β^+	0.185 (44)	0.183 (10)	0.1896 (19)
This work	*0.171*	*0.174*	*0.164*	*0.167*	*0.193*

1. M shell contribution not given.

3.3 Discussion

Results under different assumptions for Bahcall's and Vatai's approaches are given in the Tables. In principle, Vatai's approach should be more reliable and indeed, a slightly better

accuracy is observed if the hole and shaking effects are taken into account. However, the relevance of this statement is strongly limited by the precision of the measurements. As expected, the relative capture probability ratios are more sensitive to the hole effect than to the shaking correction, while the latter has a significant influence on the capture-to-positron ratios in Vatai's approach.

Except for ^{55}Fe and ^{138}La, the present modelling does not provide more accurate results than the LogFT program, while additional effects have been incorporated. This is essentially due to the high sensitivity of the capture probabilities to the exactness of the atomic wave functions in the vicinity of the nucleus. Although LogFT does not correct for hole and shaking effects, a correction of the overlap and exchange effects is included in the tabulated values used by the program but according to Bahcall's original approach (K, L_1 and M_1 subshells only). In addition, these tabulated values were determined using very accurate atomic wave functions from relativistic Hartree-Fock-Slater calculations with a realistic Fermi-Dirac distribution for the nuclear charge density. It was not possible in this work to use these tabulated values because the additional effects incorporated in the present modelling require the computation of overlaps, thus the wave functions with their spatial extension. The wave functions are alternatively determined with a home-made code based on Behrens and Bühring, (1982) formalism with the nuclear charge density taken as a uniformly charged sphere, and with atomic energies from relativistic Dirac-Fock calculations (Desclaux, 1973).

Significant improvement can therefore be expected using the present modelling with Vatai's approach and atomic wave functions of high accuracy. Their spatial extension is necessary to determine all the involved overlaps, which excludes any simple table of parameters. The self-consistent approach would increase the exactness of the hole effect compared to the use of first order perturbation theory, and would also be beneficial to the

shaking correction whose accuracy is of importance for the determination of the capture-to-positron ratios.

3.4 Application to ^{40}K decay

The present modelling was applied to the ^{40}K decay. This radionuclide can decay by a third forbidden unique beta minus transition to the ground state of ^{40}Ca, by a first forbidden unique electron capture transition to the first excited state (1460 keV) of ^{40}Ar, and by electron capture or beta plus emission to the ground state of ^{40}Ar, which is a third forbidden unique transition. The decay rate to the ground state of ^{40}Ar has not been reported in the literature. In a recent study, the interpretation of the results from the DAMA experiment in terms of Dark Matter models has been suspected to be very sensitive to this particular decay rate due to the ^{40}K contribution to the background (Pradler et al., 2013).

The most recent nuclear data evaluation for this radionuclide is from DDEP (Bé et al., 2010) and the Comments file (Mougeot and Helmer, 2009) depicts the procedure and provides every measured value of interest. The decay scheme was built upon the following probability ratios: *i*) $P_{\varepsilon,1460}/P_{\beta^-} = 0.1182\ (12)$ determined from the ratio of the corresponding partial half-lives; *ii*) $P_{\beta^+}/P_{\beta^-} = 1.12\ (14) \cdot 10^{-5}$ which comes from a single measurement (Engelkemeir et al., 1962); and *iii*) $P_{\varepsilon,g.s.}/P_{\beta^+} = 200\ (100)$. The latter ratio was determined using the LogFT program, although the code cannot calculate directly such third forbidden unique transitions. Hence, the evaluator estimated this ratio by extrapolating that calculated for a first forbidden unique transition, i.e. $P_{\varepsilon,gs}/P_{\beta^+} = 8.51\ (9)$, and that calculated for a second forbidden unique transition, i.e. $P_{\varepsilon,g.s.}/P_{\beta^+} = 45.20\ (47)$, and assuming that this ratio rises by the same factor for a third forbidden unique transition, rounding to the first significant digit and extending the uncertainty to 50% of the value.

The improved modelling of the present work can calculate exactly this third forbidden unique transition. Using the most recent Q-value of 1504.40 (6) keV, one obtains $P_{\varepsilon,g.s.}/P_{\beta+} = 215.0\ (31)$ as the mean value of 212.02 (15) from Bahcall's approach and 217.93 (15) from Vatai's approach (see Section 2.6). The corresponding capture probabilities can also be of interest and are calculated as follows: $P_K = 0.8862\ (7)$; $P_L = 0.09859\ (48)$; and $P_M = 0.01519\ (19)$. The $P_{\varepsilon,g.s.}/P_{\beta+}$ ratio is thus consistent with the originally estimated one, and leads to the following transition probabilities (compared to previous ones): $P_{\beta-} = 89.23\ (13)\%$ (versus $89.25\ (17)\%$); $P_{\varepsilon,1460} = 10.55\ (11)\%$ (identical); $P_{\varepsilon,gs} = 0.215\ (27)\%$ (versus $0.2\ (1)\%$); $P_{\beta+} = 0.00100\ (12)\%$ (identical). This new and more precise value of $P_{\varepsilon,gs}$ is a more stringent constraint for the analysis of Pradler et al. (2013) and should be taken into account in a further analysis. As the results of the DAMA experiment in the 3 keV region seem to be pivotal, it is noteworthy that a flat contribution of the beta minus spectrum from ^{40}K decay at these low energies, as taken in (Pradler et al., 2013), is not an accurate hypothesis because atomic effects, such as screening and exchange, can substantially modify the spectrum shape (Mougeot and Bisch, 2014).

During the evaluation of the total half-life of ^{40}K decay, a distinction is made between measurements that detected beta particles or gamma-rays or both in order to prevent from possible biases. In addition, the vast majority of the studies published partial half-lives, either for the beta minus branch or for the capture branch to the 1460 keV level of ^{40}Ar. To determine the total half-life of ^{40}K decay, all of these measurements have then to be consistently corrected with the corresponding transition probabilities established above. The procedure used in the DDEP evaluation was followed, leading to a consistent data set and a new half-life of $T_{1/2} = 1.2501\ (23) \cdot 10^9$ a, closed to and consistent with the previous one $T_{1/2} = 1.2504\ (30) \cdot 10^9$ a but with a lower uncertainty by 20%.

4. Conclusion

To answer a request from the decay data and radionuclide metrology communities, the calculation of electron capture transitions has been addressed on the basis of the Behrens and Bühring formalism. Allowed and forbidden unique transitions are calculated exactly, without any limitation on the transition order. Relativistic bound wave functions are determined for the atomic electrons and used for calculating the atomic effects, which are of high importance for electron captures. The overlap and exchange effects are commonly treated following Bahcall's or Vatai's approach. Both approaches were extended in the present work to every subshell in a unified formulation, taking precisely into account the occupation of the different orbitals. As Vatai's approach neglects the shaking effects, Crasemann's formulation has been used to estimate the probability of secondary vacancies for each possible captured electron. Finally, as the capture process produces the daughter atom in an excited state, the influence of the hole on the bound wave functions was estimated by means of first order perturbation theory. Relative capture probabilities and their ratios are determined for each orbital, as well as capture-to-positron ratios determined using improved beta calculations from previous work (Mougeot and Bisch, 2014). The propagation of uncertainties from the input parameters is also included. Therefore unlike LogFT, access is possible to any subshell and uncertainties are propagated for every quantity, and unlike EC-capture, the beta plus component is treated.

To validate this model, predictions have been compared to a selection of published measurements for allowed and first- and second forbidden unique transitions. Significant improvements were found for the ^{40}K, ^{55}Fe and ^{138}La decays. However in other cases, the present modelling of the electron capture leads to comparable results with the LogFT and EC-capture codes. This analysis is limited by the precision of the current measurements, not sufficient to distinguish between the theoretical predictions of the different codes, and also not sufficient to distinguish between the predictions from Bahcall's and Vatai's approaches in their

extended version as presented here. New high precision measurements are definitely required to improve the experimental data and thus the theoretical modelling. Existing discrepancies in datasets encountered for some radionuclides, e.g. ^{22}Na, should be settled with new measurements. The ^{40}K decay is of special interest for many applications and its study at low energy, particularly difficult due to the presence of three (electron capture, beta plus and beta minus) third forbidden unique transitions, is strongly recommended.

Including these calculations in the BetaShape code (Mougeot, 2017) is expected in the near future. The tabulation of certain parameters that define the wave functions would avoid the time-consuming convergence process detailed in (Mougeot and Bisch, 2014). The consistent model presented here can be improved, for example the use of self-consistent relativistic wave functions for the electron bound state orbitals would allow a precise account of the vacancy due to the capture process and a better estimate of the shaking effects. Multiple exchange processes could also be considered to improve the atomic corrections. Finally, the inclusion of nuclear structure would allow the calculation of forbidden non-unique transitions.

References

Audi, G., Kondev, F. G., Wang, M., Pfeiffer, B., Sun, X., Blachot, J., MacCormick, M., 2012. The NUBASE2012 evaluation of nuclear properties. Chin. Phys. C 36, 1157-1286.

Bahcall, J. N., 1962. Effect of exchange on L to K capture ratios. Phys. Rev. Lett. 9, 500-502.

Bahcall, J. N., 1965. Exchange and overlap effects in electron capture ratios: physical basis and experimental tests. Nucl. Phys. 71, 267-272.

Bambynek, W., Behrens, H., Chen, M. H., Crasemann, B., Fitzpatrick, M. L., Ledingham, K. W. D., Genz, H., Mutterer, M., Intemann, R. L., 1977. Orbital electron capture by the nucleus. Rev. Mod. Phys. 49, 77-221.

Bé, M. M., Chisté, V., 2003. ^{204}Tl – Comments on evaluation of decay data. DDEP Collaboration. http://www.nucleide.org/DDEP_WG/Nuclides/Tl-204_com.pdf

Bé, M. M., Chisté, V., Helmer, R. G., 2005. ^{65}Zn – Comments on evaluation of decay data. DDEP Collaboration. http://www.nucleide.org/DDEP_WG/Nuclides/Zn-65_com.pdf

Bé, M. M., Chisté, V., Dulieu, C., Mougeot, X., Browne, E., Chechev, V., Kuzmenko, N., Kondev, F. G., Luca, A., Galán, M., Nichols, A. L., Arinc, A., Huang, X., 2010. Table of Radionuclides (Vol. 5 – A = 22 to 244). Monographie BIPM-5, vol. 5, Bureau International des Poids et Mesures.

Behrens, H., Bühring, W., 1982. Electron Radial Wave Functions and Nuclear Beta Decay. Clarendon, Oxford.

Broda, C., Cassette, P., Kossert, K., 2007. Radionuclide metrology using liquid scintillation counting. Metrologia 44, S36–S52.

Crasemann, B., Chen, M. H., Briand, J. P., Chevallier, P., Chetioui, A., Tavernier, M, 1979. Atomic electron excitation probabilities during orbital electron capture by the nucleus. Phys. Rev. C 19, 1042-1046.

Desclaux, J. P., 1973. Relativistic Dirac-Fock expectation values for atoms with Z=1 to Z=120. Atomic Data and Nuclear Data Tables 12, 311-406.

Engelkemeir, D. W., Flynn, K. F., Glendenin, L. E., 1962. Positron emission in the decay of ^{40}K. Phys. Rev. 126, 1818-1822.

Firestone, R. B., McHarris, W. M., Holstein, B. R., 1978. Interpretation of the anomalous electron-capture to positron decay ratio in ^{22}Na. Phys. Rev. C 18, 2719-2726.

Galán, M., 2009. ^{22}Na – Comments on evaluation of decay data. DDEP Collaboration. http://www.nucleide.org/DDEP_WG/Nuclides/Na-22_com.pdf

Gove, N. B., Martin, M. J., 1971. Log-f Tables for Beta Decay. Nucl. Data Tables 10, 205-317.

Kellett, M. A., Bersillon, O., 2017. The Decay Data Evaluation Project (DDEP) and the JEFF-3.3 Radioactive Decay Data Library: Combining International Collaborative Efforts on Evaluated Decay Data. To be published in the Proceedings of the International Conference on Nuclear Data for Science and Technology (ND2016), Bruges, Belgium, 11-16 September 2016.

LogFT program, 2001. http://www.nndc.bnl.gov/nndcscr/ensdf_pgm/analysis/logft/. Original code from (Gove and Martin, 1971).

Loidl, M., Rodrigues, M., 2017. Direct measurement of the electron capture probability ratios of ^{55}Fe. Applied Radiation and Isotopes (this issue).

Lu, C. C., Carlson T. A., Malik F. B., Tucker, T. C., Nestor Jr, C. W., 1971. Relativistic Hartree-Fock-Slater eigenvalues, radial expectation values, and potentials for atoms, $2 \leq Z \leq 126$. Atomic Data 3, 1-131.

Martin, M. J., Blichert-Toft, P. H., 1970. Radioactive atoms: Auger electron, α-, β-, γ- and X-ray Data. Nuclear Data Tables A8, 1-198.

Messiah, A., 1995. Mécanique quantique. Dunod, chap. XVI p. 590.

Mougeot, X., Helmer, R. G., 2009. ^{40}K – Comments on evaluation of decay data. DDEP Collaboration. http://www.nucleide.org/DDEP_WG/Nuclides/K-40_com.pdf

Mougeot, X., Bisch, C., 2014. Consistent calculation of the screening and exchange effects in allowed β^- transitions. Phys. Rev. A 90, 012501.

Mougeot, X., 2017. BetaShape: A new code for improved analytical calculations of beta spectra. To be published in the Proceedings of the International Conference on Nuclear Data for Science and Technology (ND2016), Bruges, Belgium, 11-16 September 2016.

NNDC, 2017. Bhat, M.R. in Evaluated Nuclear Structure Data File (ENSDF), edited by S. M. Qaim, Nucl. Data Sci. Tech. (Springer-Verlag, Berlin, 1992), p. 817. Data extracted using

the NNDC On-Line Data Service from the ENSDF database, files revised as of February 2017. See https://www.nndc.bnl.gov/ensdf/

Pradler, J., Singh, B., Yavin, I., 2013. On an unverified nuclear decay and its role in the DAMA experiment. Phys. Lett. B 720, 399-404.

Pritychenko, B., Běták, E., Kellett, M. A., Singh, B., Totans, J., 2011. The Nuclear Science References (NSR) database and Web Retrieval System. Nucl. Instr. Meth. Phys. Res. A 640, 213-218.

Quarati, F. G. A., Dorenbos, P., Mougeot, X., 2016. Experiments and theory of ^{138}La radioactive decay. Appl. Radiat. Isot. 109, 172-176.

Samworth, E. A., Warburton, E. K., Engelbertink, G. A. P., 1972. Beta decay of the ^{26}Al ground state. Phys. Rev. C 5, 138-142.

Schönfeld, E., 1998. Calculation of fractional electron capture probabilities. Appl. Radiat. Isot. 49, 1353-1357.

Vatai, E., 1970. On the exchange and overlap corrections in electron capture. Nucl. Phys. A 156, 541-552.

Wang, M., Audi, G., Kondev, F. G., Huang, W. J., Naimi, S., Xu, X., 2017. The AME2016 atomic mass evaluation. Chin. Phys. C 41, 03003.